Inclination angle influence on noise of cavitating marine propeller

Sakir Bal[*]

Department of Naval Architecture and Marine Engineering, Istanbul Technical University, Istanbul, Turkey

Abstract. In this study, the effects of inclined shaft angle on the hydro-acoustic performance of cavitating marine propellers are investigated by a numerical method developed before and Brown's empirical formula. The cavitating blades are represented by source and vortex elements. The cavity characteristics of the blades such as cavitation form, cavity volume, cavity length etc., are computed at a given cavitation number and at a set advance coefficient. A lifting surface method is applied for these calculations. The numerical lifting surface method is validated with experimental results of DTMB 4119 model benchmark propeller. After calculation of hydrodynamic characteristics of the cavitating propeller, noise spectrum and overall sound pressure level (OASPL) are computed by Brown's equation. This empirical equation is also validated with another numerical results found in the literature. The effects of inclined shaft angle on thrust coefficient, torque coefficient, efficiency and OASPL values are examined by a parametric study. By modifying the inclination angles of propeller, the thrust, torque, efficiency and OASPL are computed and compared with each other. The influence of the inclined shaft angle on cavity patterns on the blades are also discussed.

Keywords: propeller; cavitation; noise; hydro-acoustic; shaft inclination angle

1. Introduction

Propeller radiated noise is a significant topic that should be investigated during the preliminary design stage of ships and underwater vehicles. This topic is gaining importance from day to day for civil vehicles in terms of comfort of the passengers and marine environment as well as for military purposes (underwater detectability). Besides that, small or medium-sized naval vessels can utilize propellers on inclined shafts. The forces, torques and even cavity patterns and noise values (Overall sound pressure level, OASPL) generated by inclined shaft propellers are different to those of conventional (non-inclined) shafts. This difference gets be larger with an increase in angle of inclined shaft. Therefore, the influence of the inclined shaft on hydro-acoustic performance of cavitating propellers is significant and should be investigated in the preliminary design process of propellers.

Noise signatures of marine propellers are generally predicted by applying noise measurements in the cavitation tunnel or numerical calculations using different viscous or potential based flow solvers and empirical formulas. In the past, numerous researchers predicted both non-cavitating and

---

∗Corresponding author, Professor, E-mail: sbal@itu.edu.tr

cavitating noise of marine propellers through numerical tools and experiments. Seol and others investigated   non-cavitating noise of a single and ducted propeller using a potential based flow solver (Seol *et al.* 2002). Blade sheet cavitation noise of different marine propellers was predicted using several semi-empirical formulas (Ekinci *et al.* 2010). The authors found that semi-empirical approaches are fast, easy and also give reliable solutions with low cost for propeller noise estimation, especially in initial design stage. It was focused on propeller radiated noise and cavitation modelling for the Potsdam Propeller Test Case (PPTC) in another study (Lidtke *et al.* 2016). Model propeller noise was predicted by using RANS equations with FWH (Ffowcs Williams-Hawkings) approach at the receiver located 100 m from the shaft centerline at the propeller plane. It was shown that cavitation noise in low frequencies can be readily computed by acoustic analogy and cavitation model. Sakamoto and Kamiirisa predicted cavitation noise in near field by a viscous solver with Brown's empirical formula for four different propellers (Sakamoto and Kamiirisa 2018). It was found that the upper bound limit of broadband noise compared to experimental results can be predicted Brown's formula precisely. Sheet cavitation noise was modeled using a semi-empirical method in (Brown 1999). An experimental study for flow induced noise from a turbulent boundary layer of an underwater towed body was presented in (Abshagen *et al.* 2016). A very simple and practical approach for propeller radiated noise was also given in (Bal 2019). Semi-empirical Brown's method was utilized and the logarithmic nature of noise has been justified.

It is also well-known that the flow properties of a marine propeller with an inclined shaft is unsteady even in open water conditions. In the past, an unsteady analysis and design methods of propellers were developed in (Kerwin and Lee 1978, Kuiper and Jessup 1993). In another study, RANS (Reynolds Averaged Navier-Stokes) solver for axisymmetric flows was combined with a vortex lattice design method as in (Kerwin *et al.* 1994). Effective wake data in this study was provided for the design technique (based on vortex distributions) by using RANS equations. On the other hand, the propeller thrust was included in the RANS equations as a body force. Both the propeller analysis techniques and design methods were further improved in (Griffin and Kinnas 1998). A search methodolgy for cavity was included into the analysis method, along the blade sections. The skew distribution and minimum pressure constraints were also included into the design method. In another study, an unsteady analysis method developed by Kinnas and others (Kinnas *et al.* 1998) was extended to apply for the podded propellers succesfully (Bal and Guner 2009). An iterative technique was developed by seperating the pod part, the strut part and the propeller blades. The results of the method converged very fast and it was also suggested for other multi-component propulsor systems. Two different numerical methods (a RANS equation method and a panel method) were applied for the analysis of unsteady propeller flow under an oblique inflow condition in (Gaggero *et al.* 2010). Cavitation on the other hand was not considered in this study. RANS equations solvers were also applied for the analysis of steady and unsteady propeller performances in (Krasilnikov *et al.* 2009). RANS solver coupled with a panel method was applied for predicting the performance of contra rotating propellers in (Su and Kinnas 2017). The effects of wake modelling on propeller cavitation have been investigated experimentally under inclined shaft condition in (Tani *et al.* 2018). The accurate prediction of the unsteady propulsor forces and torques in non-uniform wakes was also modelled numerically in the preliminary design or later stages of analysis of any propulsor in (Renick 2001). However, no cavitation was included into the calculations. A systematic study comparing a RANS equations solver and a panel method for propeller analysis was presented in (Brizzolara *et al.* 2008). The effects of cavitation on propeller performance were not considered in this study. But reliability of panel method was discussed in a detailed manner. Moreover, the importance of proper design of marine propulsion systems has been

studied by a method for fishing vessels in (Manouchehrinia *et al.* 2018). In addition a recent overview of the hydrodynamic aspects of marine propellers under unsteady flow conditions was published in the book of Kerwin and Hadler (Kerwin and Hadler 2010).

In the past, a searching technique of cavity detachment point for back and mid-chord cavitation was also added in the numerical method (Kinnas *et al.* 1998, Greely and Kerwin 1982). The viscous effects were assumed to be dominant near the leading edge of the blade sections. Later, a numerical method based on (Greely and Kerwin 1982) was developed in (Szantyr 1994). This method improved significantly the cavitation simulation on the blades of the propeller (Szantyr 1994). A simpler method based on a lifting line model to compute the propeller hydrodynamic performance was also later introduced in (Celik and Guner 2006). Cavitation has been modelled by RANS equations and DES (Detached Eddy Simulation) under inclined shaft condition in (Yilmaz et al. 2017). It has been reported that this technique has improved the simulation results significantly. The wake alignment procedure that is very important for inclined shaft propeller has been investigated in (Kinnas and Pyo 1999). Characteristics of unsteady flow around cavitating propeller and propeller performance were investigated by a lifting surface method. The propeller shaft inclination was especially emphasized here. The cavitating blades of the propeller can be represented by source and vorticity elements as in (Greely and Kerwin 1982).

The loading on the blades and the vorticity distribution in the wake can be depicted by vortex elements with unknown strengths on the camber line. The blade thickness can also be taken into account for by distributing source panels on the blade surface. Strengths of singularities of vortex/source distributions are unknown. Strengths can be computed using both the kinematic and dynamic boundary conditions on the blades of propeller (Bal 2011). The present numerical method can predict the unsteady loading, steady forces and cavitation parameters on the propeller blades. This method has been applied to DTMB 4119 model propeller with Brown's formula and the effects of inclined shaft angle on the hydro-acoustic results are discussed. The original point here is to investigate the hydro-acoustic properties of a cavitating ship propeller with an inclined shaft.

2. Numerical method

2.1 Lifting surface method

The performance of a marine propeller can be predicted by the numerical (lifting surface) method developed before as similar to the one given in (Bal 2011). This method is summarized here for the completeness of the paper. The method assumes that the fluid (water) is incompressible and inviscid and the flow is irrotational. Total velocity (q) around propeller can be written as follows

$$\vec{q}\,(x, y, z, t) = \vec{U}\,(x, y, z, t) + \nabla\phi(x, y, z, t) \tag{1}$$

Here ϕ is the perturbation potential due to propeller and U is the velocity of incoming uniform flow.

The propeller blades, including wakes are discretized into elements of vortices and sources (Fig. 1). The vortex elements are located on the camber lines of blade sections. There is also a source of distribution to represent the effect of blade thickness on the flow and a source lattice throughout the cavity extent to represent the cavity thickness in case of cavity. Method is known as a numerical (lifting surface) method. The sources representing blade thickness are line sources along spanwise direction. The strengths of the line sources are given in terms of derivatives of the thickness in the

chordwise direction (Griffin and Kinnas 1998). Both unknown bound vortices on the blade and unknown cavity sources are determined by applying the kinematic and dynamic boundary conditions. The kinematic boundary condition is given as

$$\frac{\partial \phi}{\partial n} = -\vec{U}_{in} \cdot \vec{n} \tag{2}$$

where $\vec{n}$ is the surface unit normal vector to the mean camber surface at the control point, $\vec{U}_{in}$ is the inflow velocity with respect to the propeller fixed coordinate system and ϕ isthe perturbation potential.

According to this method, there are two types of vortices located on the blades: (i) bound vortices and (ii) wake vortices. Bound vortices are distributed in the span-wise (radial) direction of the propeller. They are for loading on the blades. The wake vortices are on the other hand, distributed in the direction of the flow. They are for induced drag. The discretized equation can then be written as in the following form

$$\sum_{\Gamma} \Gamma \, \vec{v}_\Gamma \cdot \vec{n}_m = -\vec{v}_{in} \cdot \vec{n}_m - \sum_{Q_B} Q_B \, \vec{v}_Q \cdot \vec{n}_m - \sum_{Q_c} Q_C \, \vec{v}_Q \cdot \vec{n}_m \tag{3}$$

Here, $\vec{v}_\Gamma$ and $\vec{v}_Q$ are the velocity vectors induced by each vortex and source elements which have unit strengths, respectively. $\vec{n}_m$ is the normal (to the wake surface) vector and has a unit magnitude. Q_B and Q_C represent the magnitude of the line sources that model the blade thickness and cavity source strengths, respectively. The kinematic boundary condition must be satisfied at certain control points located on the blade mean camber surface. The kinematic boundary condition requires that the sum of the influences for all of the vortices, sources and inflow normal to a particular control point on the blade is equal to zero. Another way to explain this is that the kinematic boundary condition requires the flow to be tangent to the surface. The dynamic boundary condition is based on Bernoulli's equation between a point far from the propeller and the point of interest. This condition is defined as given by (Griffin and Kinnas 1998)

$$p - p_{shaft} = -\rho \frac{\partial \phi}{\partial t} - \rho u V_r - \rho g y_s \tag{4}$$

where p is the pressure at the point of interest, p_{shaft} is the pressure at a point far from the propeller at the depth of the shaft axis, ρ is the density of water $\frac{\partial \phi}{\partial t}$ is the time derivative of the potential induced by all of the singularities, u is the perturbation velocity along the chordwise direction, V_r is the unperturbed velocity with respect to the propeller system and y_s is the hydrostatic depth of the point of interest.

The dynamic boundary condition requires that the pressure must be equal to vapor pressure at control points covered by the cavity. The area of application of the dynamic boundary condition changes with time as the cavity extent changes with time. The unknown cavity extent is determined by searching for the cavity length along each spanwise location. The desired cavity length is the one which renders the cavity pressure equal to vapor pressure. The pressures on the cavity and blade are evaluated via Bernoulli's equation with the three-dimensional linearized velocity terms, the

unsteady terms $\dfrac{\partial \phi}{\partial t}$, and the hydrostatic terms fully included. The cavity thickness (thus volume)
is determined by integrating the cavity source distribution over the cavity surface along each strip.
The problem is solved in the time domain with each time step representing an angular rotation of
the propeller. The time domain solution allows for the effects of all strips and blades to be accounted
for in an iterative fashion. After the first complete propeller revolution, the method achieves the
fully wetted steady solution. Three more propeller revolutions produce the fully wetted unsteady
solution. Finally the cavitating unsteady solution is attained after a total of seven or more propeller
revolutions. Refer to Griffin and Kinnas (2001) for details.

Other assumptions employed throughout the method include:

    i)   The cavity thickness varies linearly across panels in the chordwise direction and is
             piecewise constant across panels in the spanwise direction,

    ii)   There are no spanwise flow effects in the cavity closure condition,

    iii)   Viscous force is calculated by applying a uniform frictional drag coefficient, C_f on the
             wetted regions of the blade. Note also that when the skin friction is computed over the
             blades, the cavity area is excluded from wetted region.

The induced velocities due to vortex elements of the lifting surface are on the other hand
calculated using Biot-Savart's law expressed as

$$\vec{V}_\Gamma = \frac{\Gamma}{4\pi} \cdot \frac{\vec{L} x \vec{d}}{\vec{d}^3}$$

(5)

where $\vec{V}_\Gamma$: induced velocity, Γ: circulation, $\vec{L}$: vortex length element, $\vec{d}$: distance between the
element and the field point. The induced velocities due to sources/sinks are also computed on the
basis of given source/sink intensity. Once the bound vortex elements intensity is solved, then the
velocity induced by the propeller in any point in space can be computed using angular positions of
the propeller blade. The forces on the propeller blade are found by the law of Kutta-Joukowsky. The
contributions of all lattice elements to the total forces are added along the blades. If the propeller is
working in a steady state condition, the forces on all blades are same. Hence, the force on the entire
propeller is found by multiplying each blade force by the number of blades. Hub effect using the
method of images can also be included into the calculations. Refer to Kerwin (2001), Griffin and
Kinnas (1998) and Bal and Guner (2009) for details of the lifting surface method.

In this numerical method, the cavity shape (formation) can also be calculated instantaneously. If
the pressure drops under the vapor pressure of water, the cavitation occur. The method assumes that
the cavity initiates at the leading edge of the corresponding section. It is also assumed that there is
a linear cavity thickness variation thorough every cavity panel. Cavity panels are located in the
chord-wise direction of sections. First the strengths of bound vortices are found and then the velocity
induced by the singularities on the blades can be computed by using angular positions of propeller
blades. The average value is taken as the induced velocity by the propeller. Both laws of Kutta-
Joukowsky and Lagally are then used for the forces acting on the vortices and sources, respectively
(Kerwin and Lee 1978). A wake alignment scheme in the case of inclined flow is applied to get a
force-free wake surface. Trailing vortex wake is assumed to be changed with blade angle. For details
of wake alignment, refer to (Kinnas and Pyo, 1999). The inclination angle (δ) of propeller shaft is
shown in Fig. 2. Note also that the non-linear leading edge corrections have been included in the
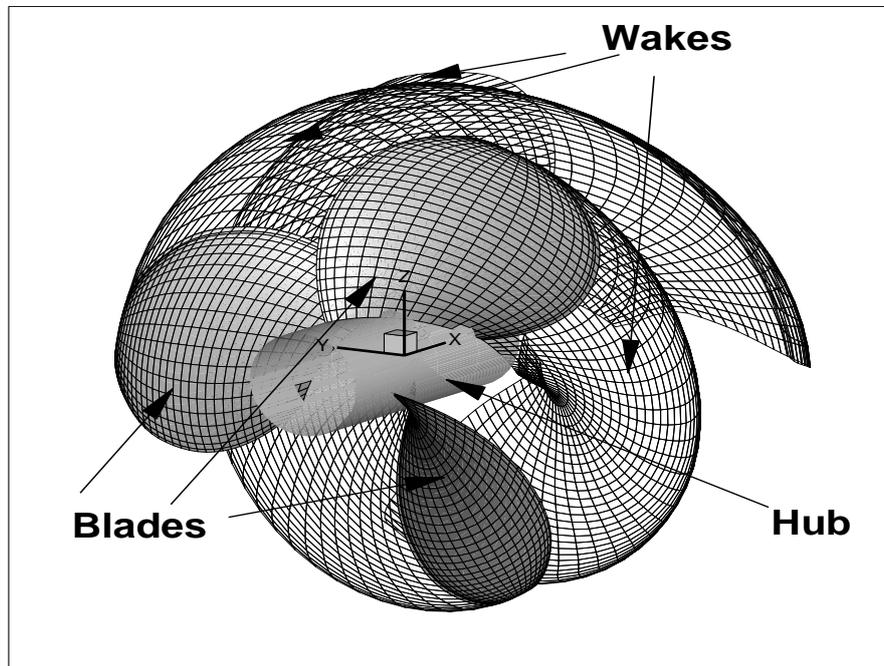
Fig. 1 Panels on blades, wakes of propeller and definition of coordinate system
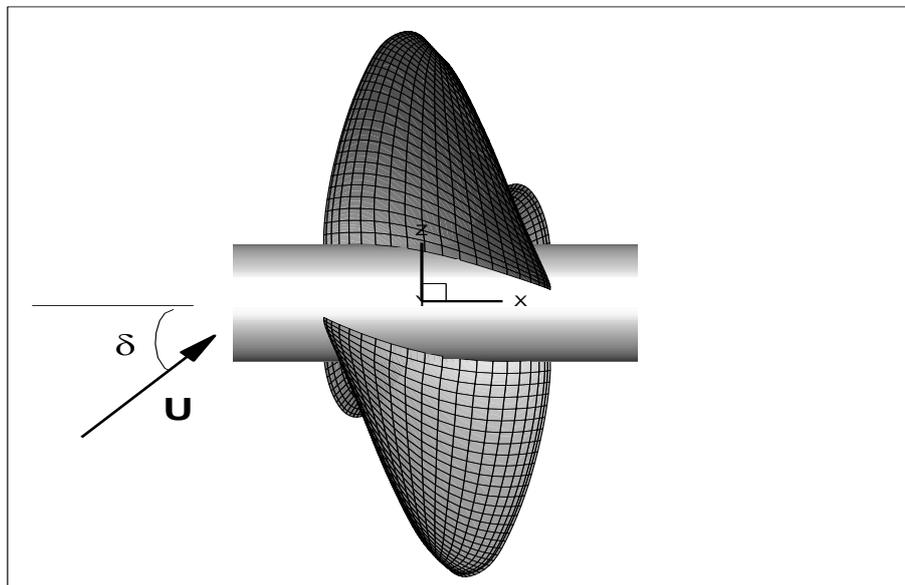
Fig. 2 Definition of shaft inclination angle

calculations as given in (Kinnas 1991). Refer to (Bal 2011) for details on the numerical method used for the analysis problem.

2.2 Brown's empirical formula

Empirical Brown's formula based on broadband noise estimation has been applied here as given in (Yoshimura and Koyanagi 2004). This approach is used to calculate the total sound pressure level (SPL) at the reference distance of 1 meter in z direction above the shaft axis. SPL has been given in the following equation as follows:

$$SPL = 105 + 10 \ log_{10} \left(\frac{ZD^4 n^3}{f^2} \right) + 10 \ log_{10} \left(\frac{A_C}{A_0} \right) \qquad (3)$$

Here, Z is the blade number, D is the diameter of the propeller (in meters) and n is the propeller rotation speed (number of revolutions per second) while f is the noise frequency (in Hz). A_C and A_0 are the maximum swept cavity area and propeller disc area (in m^2), respectively. SPL represents the noise level in dB. SPL is by definition,

$$SPL = 10 \ log_{10} \left(\frac{p}{p_{ref}} \right)^2 \qquad (4)$$

where p is the acoustic pressure (Pa) and p_{ref} is the reference acoustic pressure (for water $p_{ref}=10^{-6}$ Pa). Overall sound pressure level (OASPL) can then be computed by,

$$OASPL = 10 \ log_{10} \left(\frac{p_{rss}}{p_{ref}} \right)^2 \qquad (5)$$

Here, p_{rss} is the square root of the sum of the pressure levels squared (NASA 1996).

3. Results and discussion

3.1 Results of non-cavitating propeller and validation

First non-cavitating DTMB 4119 model propeller has been selected to validate the numerical (lifting surface) method (Bal 2011, Carlton 2012). The propeller inflow is uniform and there is no inclined shaft ($\delta = 0^o$). The propeller is three bladed. The diameter (D) of model propeller is 0.3048 m and the ratio of hub to diameter is 0.2. The blades of the model propeller have NACA 66 modified sections and a = 0.8 (modified) mean line. There is no skew and no rake for the propeller. The blade geometries are taken from reference (Bal 2011) and are given in Table 1.

The number of vortex elements is 20 in the chord-wise direction and 30 in the radius direction of the blade. These number of panels have been found to obtain converged results after some numerical tests. The frictional drag coefficient of whole section was assumed to be $C_f=0.0035$ in the calculations. It has been found after many numerical calculations (Kinnas *et al.* 1998). The front view of the DTMB 4119 model propeller and the panels used on the blades are shown in Fig. 3.

The thrust coefficient and torque coefficient (K_T and K_Q) and the efficiency value ($\eta = \dfrac{J}{2\pi} \dfrac{K_T}{K_Q}$)

versus the advance coefficient (J) computed from the analysis are compared with experiments and shown in Fig. 4. There is a very good agreement between the results of this analysis method and experiments. For the validation of noise values, the results of Brown's formula have been compared with those of the method given in (Seol *et al.* 2005) computed the noise spectrum of DTMB 4119

model propeller by a potential based flow solver. Inflow velocity and rotational speed of the propeller are U=1.6 m/s and n=2 rps, respectively. The receiver is located at a distance of 10R in the propeller plane above the shaft axis. The correction of the distance for Brown's method is done according to ITTC recommendation (ITTC 2014). Sound pressure levels can be corrected to a standard measuring distance of 1 m by using Eq. (6) (ITTC, 2014)

$$SPL_s = SPL_p + 20\log_{10}\left(\frac{d}{d_{ref}}\right) \tag{6}$$

Table 1 DTMB 4119 propeller geometry from (Bal 2011)

r/R	c/D	P/D	t_{max}/c	f_{max}/c
0.20	0.3200	1.1050	0.2055	0.0143
0.30	0.3635	1.1022	0.1553	0.0232
0.40	0.4048	1.0983	0.1180	0.0230
0.50	0.4392	1.0932	0.0902	0.0218
0.60	0.4610	1.0879	0.0696	0.0207
0.70	0.4622	1.0839	0.0542	0.0200
0.80	0.4347	1.0811	0.0421	0.0197
0.90	0.3613	1.0785	0.0332	0.0182
0.95	0.2775	1.0770	0.0323	0.0163
0.98	0.2045	1.0761	0.0321	0.0145
1.00	0.0800	1.0750	0.0316	0.0118
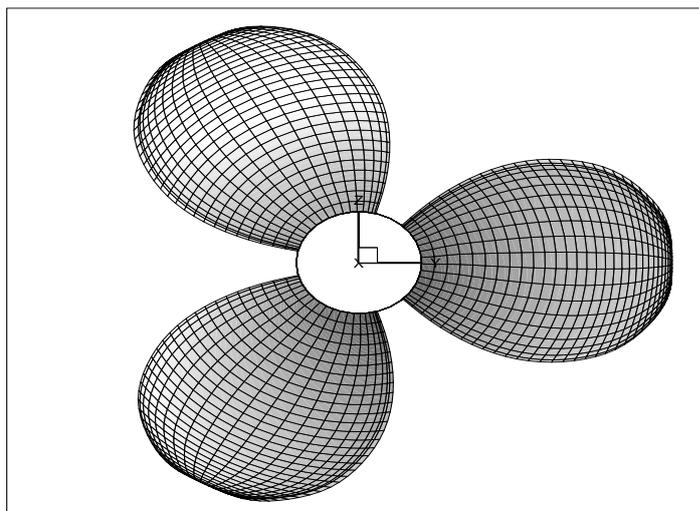
Fig. 3 Geometry and panels used on DTMB 4119 propeller
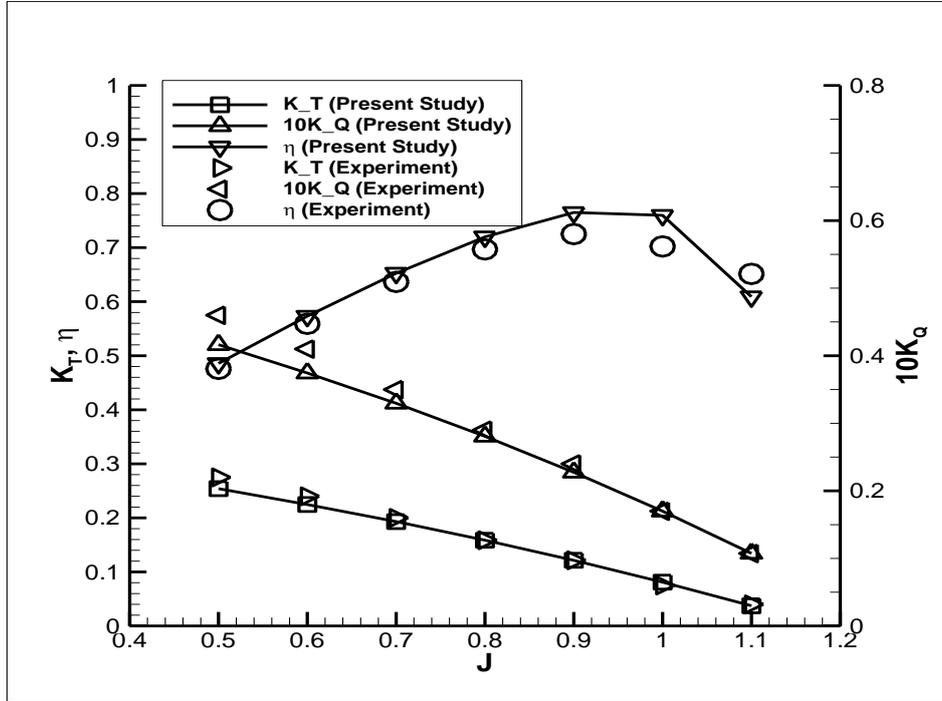
Fig. 4 Comparison of K_T, K_Q and η values with experiments (DTMB 4119)

Here, SPL_p (dB) is the reference noise level and SPL_s (dB) is the normalized noise level. d_{ref} is taken as 1 meter (Sezen and Bal 2019). Fig. 5 shows the SPL values in dB versus frequency (Hz) by Brown's formula and the method given in (Seol *et al.* 2005). Both results are in good agreement except very low frequencies (f < 30 Hz). A coefficient of 105 is then used on the right hand side of Eq. (3). Note that OASPL levels by both methods (the method given in (ITTC 2014) and the present method) are same.

3.2 Results of cavitating propeller

Same method is then used for cavitating DTMB 4119 model propeller. Advance coefficient is J = 0.8 and the cavitation number is selected as σ = 1.2. The cavitation number is defined as

$$\sigma = \frac{p - p_v}{0.5\rho(nD)^2} \tag{7}$$

Here, p is the static pressure on the shaft of the propeller and p_v is the vapour pressure. The computed cavitation patterns on all blades for the three different shaft inclination angles (δ = 0º, 5º and 10º) are shown in Figs. 6- 8, respectively. As you can see from these figures, an increase in inclination angle causes a decrease in the area covered by cavitation on the blade in the top (upper) position while an increase on the blade in the bottom (lower) position. This phenomenon is expected since the blade in the bottom position meets the flow first in inclined shaft conditions. A similar effect can also occur for the rake factor of propeller. If the rake increases in the backward direction,

the cavity formation on the blades will decrease or vice versa (Kerwin and Hadler 2010). On the other hand, increasing inclination angle causes a decrease in the thrust and torque coefficients while there is almost no change in efficiency values as shown in Table 2.
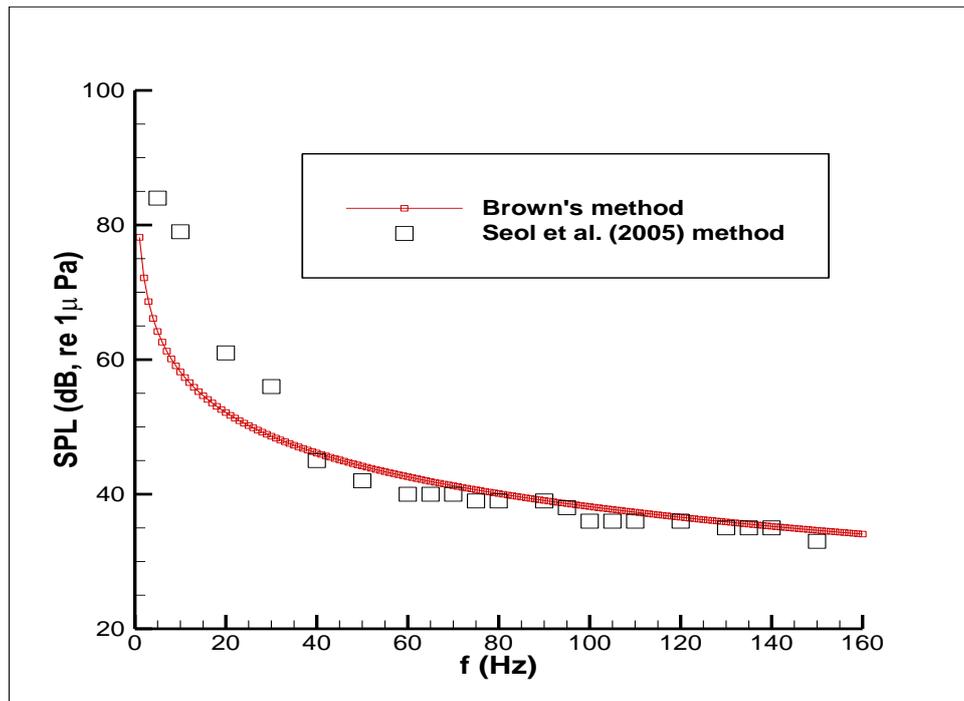
Fig. 5 Comparison of SPL by Brown's method and the method given in (Seol *et al.* 2005)
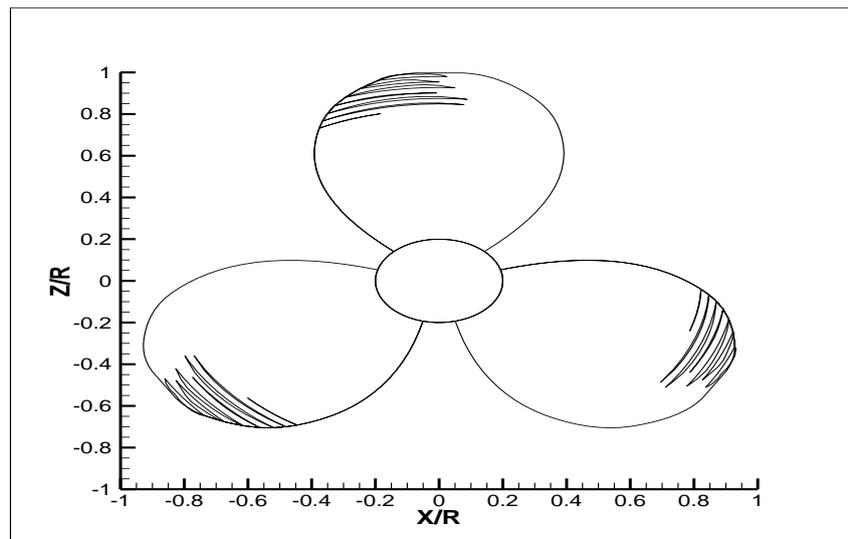
Fig. 6 Cavitation pattern on blades for J=0.8, σ=1.2 and δ=0°
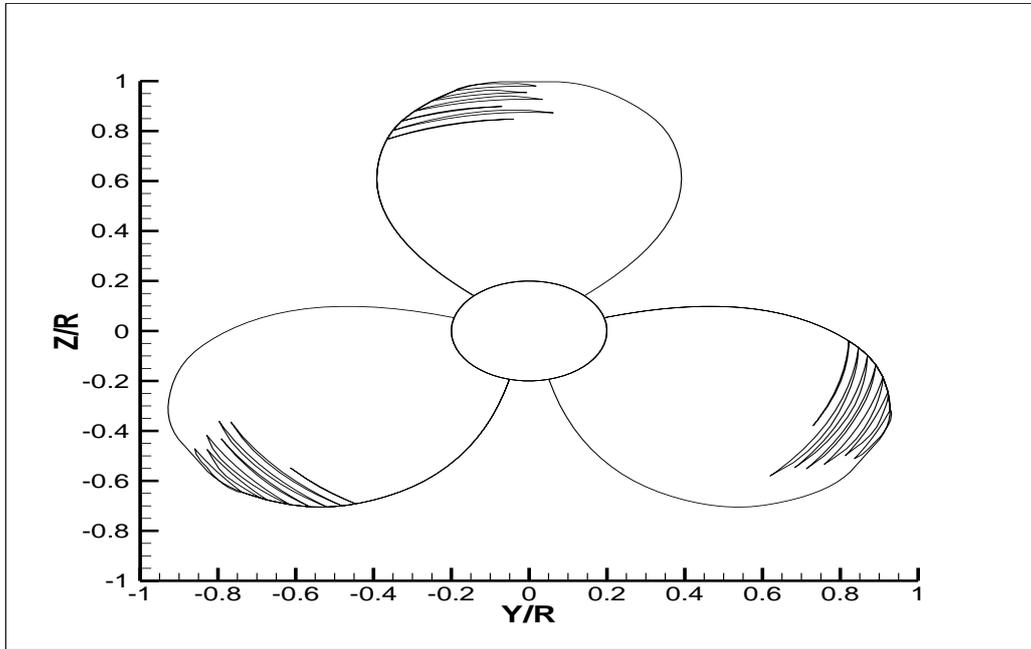
Fig. 7 Cavitation pattern on blades for J=0.8, σ=1.2 and δ=5⁰
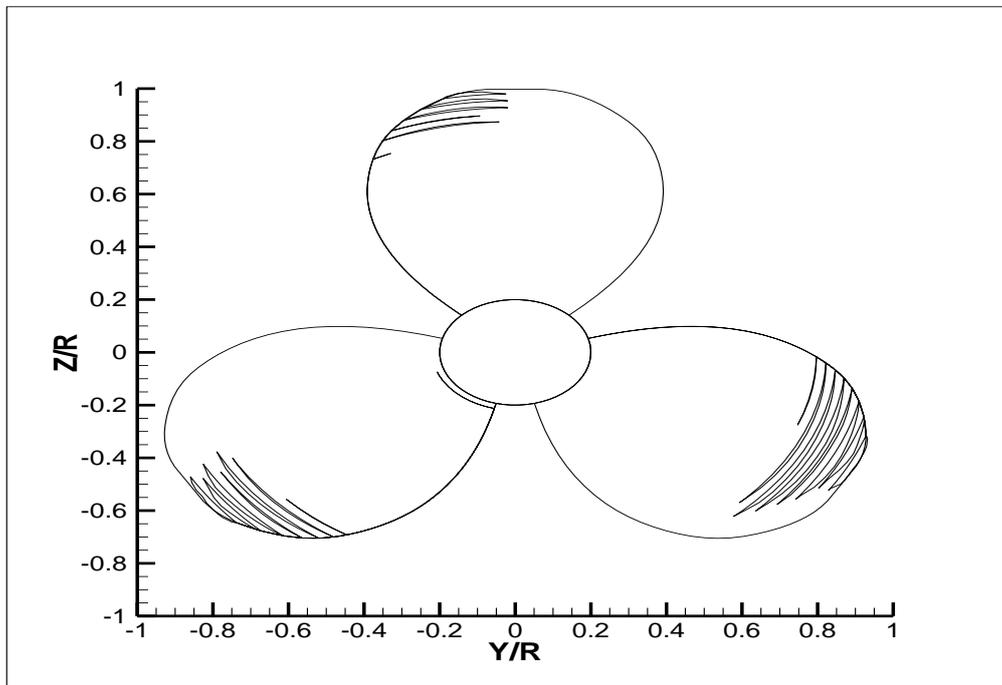
Fig. 8 Cavitation pattern on blades for J=0.8, σ=1.2 and δ=10⁰

Table 2 Thrust and torque coefficients and efficiency values versus inclination angle (J=0.8, σ=1.2)

δ (º)	0	5	10
K_T	0.1672	0.1603	0.1586
$10K_Q$	0.2961	0.2826	0.2801
η (%)	71.9	72.2	72.1

Table 3 OASPL versus inclination angle for the same thrust coefficient (K_T=0.1672, σ=1.2)

δ (º)	0	5	10
n (rps)	6.2	6.5	6.8
OASPL (dB)	104	104.5	105
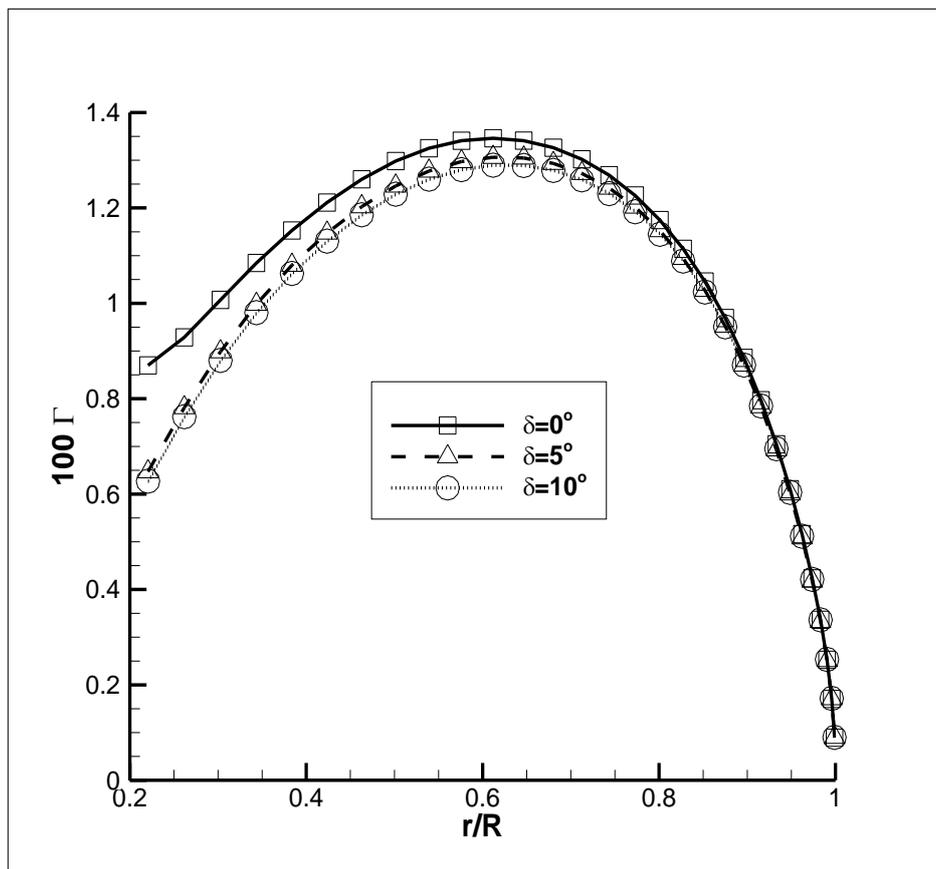
Fig. 9 Average circulation (loading) distribution on blades versus fractional radius for different shaft angles (J=0.8, σ=1.2)

Note that thrust is always parallel to the shaft. Note also that in Fig. 6, all cavity formations on all blades are the same since the incoming flow is uniform and the inclination angle for this case is equal to zero. The hydrostatic pressure has computed on the shaft axis and negligible effect on the blades. In Fig. 9, the average loading (circulation) distribution versus inclination angle of propeller shaft is shown. It is clear that the loading particularly near the root region is decreasing with an increase in inclination shaft angle. This confirms the results given in Table 2. On the other hand, there is no change on loading near the tip region with an increase in inclined shaft angle. OASPL values versus inclination angle have also been computed by equations (3-5) for the same thrust coefficient (K_T=0.1672). The receiver distance is 10R from the shaft axis in the propeller plane. The results are shown in Table 3. Note that higher inclination angles cause higher OASPL values for the same thrust coefficient. If the inclination angle increases, the thrust coefficient decreases as shown in Table 2. In order to obtain the same thrust coefficient, the rotational speed must be increased. This increase causes a higher noise level.

4. Conclusions

In this study the effects of changing the inclination angle on the noise of cavitating propellers under open water conditions have been investigated by a numerical lifting surface method and Brown's empirical formula. The DTMB 4119 propeller has been chosen for validation of the numerical method. The findings can be summarized as follows:

1-) An increase in inclination angle results in a decrease in loading (thrust and torque coefficients) on the blades of propeller under cavitating condition.

2-) An increase in inclination angle is causing no change in efficiency of the propeller under cavitating condition.

3-) An increase in inclination angle of the shaft results in a decrease in cavity length on the sections when the blade is in the top (upper) while it causes an increase when the blade is in the bottom (lower).

4-) An increase in inclination angle causes higher noise levels for the same thrust coefficient. This is mainly due to higher rotational speeds.

The approach described here can be applied for different types of propellers in a systematic way. Main parameters (number of blades, pitch ratio, blade area ratio, skew, rake etc.) of propeller can be changed systematically and hydro-acoustic values can then be computed with the effects of inclination angle very quickly. The propeller can also work under a nominal wake condition. This is under study.

References

Abshagen, J., Kuter, D. and Nejedl, V. (2016), "Flow induced interior noise from a turbulent boundary layer of a towed body", *Adv. Aircraft Spacecraft Sci. Int. J.*, **3**(1), 259-269.

Bal, S. (2011), "A practical technique for improvement of open water propeller performance", *Proceedings of the Institution of Mechanical Engineers, Part M, Journal of Engineering for the Maritime Environment*, **225**, 375-386.

Bal, S. and Guner, M. (2009), "Performance analysis of podded propulsors", *Ocean Eng.*, **36**(8), 556-563.

Brizzolara, S., Villa, D. and Gaggero, S. (2008), "A Systematic Comparison Between RANS and Panel Methods for Propeller Analysis", *Proceedings of the 8th International Conference on Hydrodynamics*,

Nantes, France.

Brown, N. (1999), "Thruster Noise", *Paper presented at Design Session of Dynamic Positioning Conference.*

Carlton, J.S. (2012), *Marine Propellers and Propulsion,* Oxford: Elsevier (Butterworth-Heinmann) Publication.

Celik, F. and Guner, M. (2006), "Improved lifting line method for marine propeller", *Marine Technol.*, **43**, 100-113.

Ekinci, S., Celik, F. and Guner, M. (2010), "A practical noise prediction method for cavitating marine propellers", *Brodogradnja*, **61**, 359-366.

Gaggero, S., Villa, D. and Brizzolara, S. (2010), "RANS and panel method for unsteady flow propeller analysis", *J. Hydrodynamics*, **22**(5), 564-569.

Greely, D.S. and Kerwin, J.E. (1982), "Numerical methods for propeller design and analysis in steady flow", *T. SNAME*, **90**, 415-453.

Griffin, P.E. and Kinnas, S.A. (1998), "A design method for high-speed propulsor blades", *J. Fluids Eng.*, **120**, 556-562.

ITTC (International Towing Tank Conference) (2014), *Guideline of Specialist Committee on Hydrodynamic Noise*. Denmark: ITTC Publications.

Kerwin, J.E. and Hadler, J.B. (2010), *Principles of Naval Architecture Series: Propulsion,* Society of Naval Architects and Marine Engineers (SNAME) Publications, Virginia, USA.

Kerwin, J.E. and Lee, C.S. (1978), "Prediction of steady and unsteady marine propeller performance by numerical lifting surface theory", *T. SNAME*, **86**, 218-258.

Kerwin, J.E., Keenan, D.P., Black, S.D. and Diggs, J.D. (1994), "A coupled viscous/potential flow design method for wake-adapted, multi-stage, ducted propulsors using generalized geometry", *T. SNAME*, **102**, 23-56.

Kinnas, S.A. (1991), "Leading-edge corrections to the linear theory of partially cavitating hydrofoils", *J. Ship Res.*, **35**(1), 15-27.

Kinnas, S.A. and Pyo, S. (1999), "Cavitating propeller analysis including the effects of wake alignment", *J. Ship Res.*, **43**, 38-47.

Kinnas, S.A., Griffin, P., Choi, J.K. and Kosal, E.M. (1998), "Automated design of propulsor blades for high-speed ocean vehicle applications", *T. SNAME*, **106**, 213-240.

Krasilnikov, V.I., Zhang, Z. and Hong, F. (2009), "Analysis of unsteady blade forces by RANS", *Paper presented at the First International Symposium on Marine Propulsors, Trondheim, Norway*.

Kuiper, G. and Jessup, S.D. (1993), "A propeller design method for unsteady conditions", *T. SNAME*, **101**, 247-273.

Lidtke, A.K., Humphrey, V.F. and Turnock, S.R. (2016), "Feasibility study into a computational approach for marine propeller noise and cavitation modelling", *Ocean Eng.,* **120**, 152-159.

Manouchehrinia, B., Molloy, S., Dong, Z., Gulliver, A. and Gough, C. (2018). "Emission and life-cycle cost analysis of hybrid and pure electric propulsion systems for fishing boats", *J. Ocean Technol.*, **13**(2), 64-87.

NASA (National Advisory of Space Agency) (1996), *Acoustic Noise Requirement.* California: NASA Publications, No: PD-ED-1259.

Renick, D. H. (2001), "Unsteady Propeller Hydrodynamics", PhD Dissertation, Massachusetts Institute of Technology, Cambridge, MA, USA.

Sakamoto, N. and Kamiirisa, H. (2018), "Prediction of near field propeller cavitation noise by viscous CFD with semi-empirical approach and its validation in model and full scale", *Ocean Eng.*, **168**, 41-59.

Seol, H., Jung, B., Suh, J.C. and Lee, S. (2002), "Prediction of non-cavitating underwater propeller noise", *J. Sound Vib.*, **257**(1), 131-156.

Seol, H., Suh, J.C. and Lee, S. (2005), "Development of hybrid method for the prediction of underwater propeller noise", *J. Sound Vib.,* **288**(1-2), 345-360.

Sezen, S. and Bal, S. (2019), "A Computational investigation of noise spectrum due to cavitating and non-cavitating propellers", *Proceedings of the Institution of Mechanical Engineers, Part M, Journal of Engineering for the Maritime Environment*, DOI: 10.1177/1475090219892368, 1-14.

Soydan, A. and Bal, S. (2019), "A practical method for propeller noise", *Naval Architect, RINA,* May: 50-51.

Su, Y. and Kinnas, S.A. (2017), "A BEM/RANS interactive method for predicting contra-rotating propeller performance", *Ocean Syst. Eng.*, **7**(4), 329-344.

Szantyr, J.A. (1994), "A method for analysis of cavitating marine propellers in non-uniform flow", *Int. Shipbuild. Progress*, **41**, 223-242.

Tani, G., Viviani, M., Villa, D. and Ferrando, M. (2018), "A study on the influence of hull wake on model scale cavitation and noise tests for a fast twin screw vessel with inclined shaft", *Proceedings of the Institution of Mechanical Engineers, Part M, Journal of Engineering for the Maritime Environment*, **232**, 307-330.

Yilmaz, N., Khorasanchi, M. and Atlar, M. (2017), "An investigation into computational modelling of cavitation in a propeller's slipstream", *Proceedings of the 5th International Symposium on Marine Propulsion*, Espoo, Finland.

Yoshimura, Y. and Koyanagi, Y. (2004), "Design of a small fisheries research vessel with low level of underwater-radiated noise", *J. Marine Acoust. Soc. Japan*, **31**(3), 137-145.

MK

Nomenclature

a	: NACA camber (mean) line constant
A_C	: Cavity area
A_0	: Propeller disk area
c(r)	: Chord length along blade
C_f	: Frictional coeffcicient
d	: Receiver (hydrophone) distance from propeller
dB	: Decibel
D	: Propeller diameter
DES	: Detached eddy simulation
f	: Frequency
f_{max}	: Maximum camber of each blade section
FWH	: Ffowcs Williams-Hawkings equation
J	: Advance coefficient $=U/(nD)$
K_T	: Thrust coefficient of propeller $=T/(\rho n^2 D^4)$
K_Q	: Torque coefficient of propeller $=Q/(\rho n^2 D^5)$
n	: Propeller rotational speed [rps]
$\vec{n}_m$	: Unit vector normal to the mean camber or trailing wake surface
OASPL	: Overall sound pressure level
p	: Pressure
p_{ref}	: Reference acoustic pressure
p_v	: Vaporization pressure of water
P(r)	: Pitch of blade section
PPTC	: Postdam propeller test case
Q	: Torque absorbed by the propeller
Q_B	: Blade source strength
Q_C	: Cavity source strength
r	: Radial parameter
r_h	: Radius of hub
R	: Radius of propeller
RANS	: Reynolds Averaged Navier-Stokes
SPL	: Sound pressure level

t	: Thickness parameter for blade sections
t_{max}	: Radial distribution of the maximum thickness
T	: Propeller thrust
U	: Uniform inflow velocity
$\vec{v}_\Gamma$	: Velocity vector induced by each unit strength vortex element
$\vec{v}_Q$	: Velocity vector induced by each unit strength source element
Z	: Number of blades
δ	: Inclination angle of shaft
$\beta(r)$	: Radial distribution of pitch angle
η	: Propeller efficiency $= J/(2\pi) \cdot (K_T/K_Q)$
Γ	: Circulation
ω	: Angular velocity $= 2\pi\, n$
ρ	: Density of water
σ	: Cavitation number